Journal of Alloys and Compounds 651 (2015) 200–207

Contents lists available at ScienceDirect

Journal of Alloys and Compounds

journal homepage: http://www.elsevier.com/locate/jalcom

Is it possible the substitution of Cr cations from spinel-type oxides with bulky rare-earth cations by sol–gel auto-combustion method?

A.I. Borhan [a], P. Samoila [b], D. Gherca [a], A.R. Iordan [a], M.N. Palamaru [a, *]

[a] "Alexandru Ioan Cuza" University, Faculty of Chemistry, Iasi 700506, Romania
[b] "Petru Poni" Institute of Macromolecular Chemistry, Iasi 700487, Romania

ARTICLE INFO

Article history:
Received 20 April 2015
Received in revised form
17 August 2015
Accepted 18 August 2015
Available online 20 August 2015

Keywords:
Rare earth oxide materials
Sol–gel processes
X-ray diffraction
Phase transitions
Magnetic measurements

ABSTRACT

Rare-earth La^{3+} cations, with large ionic radii, substituted $ZnCr_{2-x}La_xO_4$ nanoparticles with x ranging from 0.0 to 0.50 were synthesized by sol–gel auto-combustion technique. Effect of La substitution on structural and magnetic properties of $ZnCr_2O_4$ spinel oxide is reported. The phase composition of the obtained powders was investigated by Fourier transform infrared spectroscopy, X-ray diffraction, and scanning electron microscopy. Magnetic measurements were made using a *SQUID magnetometer. FT-IR and* X-ray diffraction revealed the transition of spinel structure to perovskite structure because of the exchange of Zn^{2+} and La^{3+} cations among constituent A-sites. The particle size were estimated from the SEM micrographs and were found to increase with the La ions substitution from 48 to 80 nm. It was revealed from the magnetic measurements that magnetization follow a decreasing trend with substitution of Cr^{3+} ions by paramagnetic La^{3+} ions. Also, the magnetization showed a drastic decrease with increase of temperature from 2 K to 300 K because of enhanced domain pinning effect, due to the La^{3+} substitution.

1. Introduction

There is a confusion between "doping" and "substitution" terms in many research papers. In case of doping, infinitesimally small amount of some "foreign" substance occupies only the interstitial sites but never the constituent sites and may change the electronic, magnetic, thermal properties of the crystal. Substitution is the word used when replacing one element by another one at levels reaching several percents. In this case, the "foreign" substance (in any permissible amount) always occupies the constituent sites and never the interstitial sites.

Substitution with rare earth elements of the trivalent cations from the spinel oxides is a barely explored topic in the literature, although some works incorrectly uses the term substitution. Given this reality, we asked the question what happens in terms of structural and magnetic properties in case of substitution with sufficiently large amount of rare-earth cations in octahedral sites of spinel-type oxides?

Oxides with spinel structure belong to the group of strategic materials which are used in the wide area of modern technologies, due to interesting physico-chemical properties. They exhibit excellent magnetic, electric, optic, catalytic and photocatalytic properties [1–5]. In particular, zinc chromite ($ZnCr_2O_4$) spinels are commonly used as gas and humidity sensors [6–8], as catalytic materials [9,10], and as magnetic material [11].

The general formula of spinel type oxides is $(A)[B_2]O_4$, where the tetrahedral sites (A) are occupied by divalent cations (like Zn, Ni, Co,…), and the octahedral sites [B] by trivalent cations (Fe, Cr, Al,…), in a cubic structure.

$ZnCr_2O_4$ is a mixed spinel type oxide which crystallizes to face-centered cubic lattice with Fd3m space group [12]. $ZnCr_2O_4$ is a geometrically frustrated antiferromagnet with a first order transition at 12.5 K from paramagnetic phase with cubic structure to antiferromagnetic phase with tetragonal structure [13,14].

The presence of rare earth ions into the spinel structure has been reported to lead to structural distortion that induces strains in the material and to affect the electrical and magnetic properties significantly [15]. Single ion anisotropy and magnetostriction of La are very large, therefore it is of interest to investigate the effect of La on structural and anisotropy related properties of La substituted $ZnCr_2O_4$. To date, many investigations have been carried out to understand the effect of RE^{3+} doping on the properties of spinel oxide type ferrite [16,17], Ni–Mn–Cr ferrite [18], Ni–Co ferrite [19],

* Corresponding author.
E-mail address: palamaru@uaic.ro (M.N. Palamaru).

http://dx.doi.org/10.1016/j.jallcom.2015.08.152
0925-8388/

Ni–Zn ferrite [20]. Generally, in spinel oxides, the two types of cations do not usually differ greatly in size, because the spinel structure is stable only if the cations are rather medium sized and, in addition, the ionic radii of the different cations in the same compound do not dramatically differ. Hence, substitution with non-magnetic rare earth (La) in place of Cr ions in $ZnCr_2O_4$ induce lattice distortion and magnetic defect as ionic size of La is about twice higher comparable to that of Cr ions (0.615 Å for Cr^{3+} and 1.032 Å for La^{3+}, respectively) [21]. However, La ions contributes to the weakening of the tetrahedral–octahedral superexchange interactions due to its non-magnetic nature [22]. Therefore, is expected that a relatively high amount of La^{3+} in $ZnCr_2O_4$ may create lattice strain in the material and it leads to modify the magnetic properties. Also La^{3+} exhibits only in 3+ state which, theoretically, restrict it to enter into B-sites of spinel structure only. But, this can happen only in case of doping with La ions, because of large ionic radius of these cations. Therefore, doping with a percentage of 0.2, as can easily find in the literature, it is extremely difficult to control, often leading to the transition to other structures. As said above, this represents a substitution with La ions in spinel structure. Kumar et al. [23] reported the synthesis of lanthanum–cobalt ferrites of composition $CoLa_xFe_{2-x}O_4$ (x = 0, 0.1, 0.15, 0.2) by the co-precipitation method. However, in many cases, the pure spinel structure formation, for compositions with the percentage of RE greater than 0.1, is not fully confirmed. Rahman et al. [24] investigated the gadolinium (Gd) substituted cobalt ferrites with variable Gd content (x = 0.0–0.4) and reported that a secondary phase formation ($GdFeO_3$) emerges with increasing Gd content. Peng et al. [25] reported the synthesis of Pr^{3+} doped Ni–Zn ferrite with a rare-earth content ranging between 0 and 0.08. XRD diffraction patterns confirmed the formation of secondary phases of perovskite ($PrFeO_3$) at higher Pr content. Wu et al. [26] reported the preparation of nickel–zinc ferrite with lanthanum substitution with a variable La substitution content (x = 0.0–0.4). The results indicated that the perovskite phase ($LaFeO_3$) is predominantly starting with x = 0.2, and appeared in a proportion of up to 50% even from the x = 0.1. Yehia et al. [27] investigated the structural and magnetic properties of rare-earth substituted nickel ferrites, $NiFe_{1.99}R_{0.01}O_4$ (RE = Sm, Gd, Eu, and La). Authors reported that the saturation magnetization and coercivity increased with RE-substitution and appeared to be greatly affected by the nature of RE^{3+} ions. Although it was observed that the introduction of these metals in structure affects the magnetic properties, the structure did not change significantly, which means that RE occupies the interstitial positions. This confirms that there has been a doping and not a substitution. Rezlescu et al. [28] pointed out that rare-earth ions drastically affected the physical properties of substituted ferrite due to their larger ionic radius, and when rare-earth ions entered the octahedral (B-site), they could replace Fe^{3+} ions at low rare earth ion content only. In many other investigations [29–33] a modification in the structural, magnetic and electrical properties is obtained due to the addition of rare earth ions but, in some cases conflicting results are obtained. For these reasons, further detailed investigations on rare earth-substituted ferrites are needed. Therefore, the main purpose of our investigation is to study the effect of Cr^{3+} substitution with La^{3+} ions on the structural and magnetic properties of $ZnCr_2O_4$ spinel-type oxide. According to the best of our knowledge, there is a lack of detailed study on structure and magnetic properties of these nanomaterials. The properties of spinel oxides are strongly influenced by the composition and microstructure, which are sensitive to the preparation methodology used in their synthesis. The present work deals with the preparation of $ZnCr_2O_4$ substituted with bulky La cations by using sol–gel auto-combustion technique, which is a wet-chemical method for the fabrication of inorganic materials. The concurrence of these reactions leads to the formation of more and more metal-oxygen-metal bondings, catalyzed by the air moisture and traces of water presents in the solvent. Usually these reactions are completed by a conditioning step at elevated temperature in air, which can also be used to crystallize the amorphous material. The importance of the fuels used in sol–gel auto combustion processes for the preparation of spinel-type materials was already proved. In a previous study, dealing with the preparation of rare-earth doped spinels, we demonstrated that from four different combustion agents, (citric acid, tartaric acid, urea and cellulose) only citric acid and cellulose allow the pure spinel phase formation [20]. Consequently, the citric acid was selected as a combustion agent for the preparation of studied materials.

2. Experimental

The samples of the $ZnCr_{2-x}La_xO_4$ system (x = 0, 0.25, 0.50) were prepared by sol–gel auto-combustion method from high-purity starting materials. Analytical grade chromium nitrate $Cr(NO_3)_3 \cdot 9H_2O$ (99,9%, Aldrich), lanthanum nitrate and zinc nitrate solutions were mixed in stoichiometric proportions. Lanthanum nitrate and zinc nitrate were obtained in situ from La_2O_3 (99%, Sigma–Aldrich), and ZnO (99%, Sigma–Aldrich) respectively, and nitric acid (Merck) 20% solution. A solution of citric acid [$C_6H_8O_7$] (Merck) was mixed with each sample of metal nitrates mixture in 1:1 M ratio of citric acid to metallic cations, to yield finer-sized powders, possessing desirable powder characteristics. The homogeneous solutions of nitrates were transformed into gel phase on heating for 5 h at 80 °C under continuous stirring. The dried gels were gradually heated on the sand bath up to 300 °C, when the combustion was clearly observed and all the gels were converted to powders. The powders were ground and then thermally treated in two steps: up to 500 °C/7 h and up to 700 °C/7 h.

Perovskite-type oxide, $LaCrO_3$, was prepared by sol–gel auto-combustion technique, for comparison purposes. The synthesis procedure consisted in dissolving La_2O_3 (Sigma–Aldrich) into HNO_3 (20%) (Lachner) and $Cr(NO_3)_3 \cdot 9H_2O_2$ (Merck) in distilled water, taken in equimolar amounts, followed by the addition of citric acid (Merck) in order to give a molar ratio of metallic cations and citric acid of 1:1. Consequently, the as-obtained mixture was subjected to the same heat treatments as described earlier for the spinel preparation (80 °C on the water bath, 300 °C on the sand bath, and, finally, annealing at 500 °C and 700 °C for 7 h).

Infrared study of the as-prepared powders has been done using a Bruker spectrophotometer TENSOR™ 27-type with ATR cell at a resolution of 2 cm^{-1}. IR spectroscopy was used for monitoring solid phase chemical reactions and for the disappearance of the organic phase. Structure of the as-obtained powders was confirmed by X-ray diffraction (XRD) using a Bruker ASX D8 Advance diffractometer with CuK_α radiation (λ = 1.5406 Å), for 2θ ranging between 20 and 80°, at a scanning speed of 0.02°/s. The morphology and particles size analysis of the powders obtained at 700 °C were investigated by scanning electron microscopy using a Hitachi S2600N Microscope. Magnetic properties of the obtained powders were made using a *Quantum Design MPMS XL-5 SQUID magnetometer* applying a magnetic field of 60 kOe at room temperature 300 K, and 2 K respectively.

3. Results and discussion

3.1. Infrared spectra interpretation

The IR spectra, in the wavenumber range 2000–400 cm^{-1}, for $ZnCr_{2-x}La_xO_4$ (x = 0, 0.25, 0.50) and $LaCrO_3$ powders thermally treated at 700 °C, are shown in Fig. 1. There can be seen the

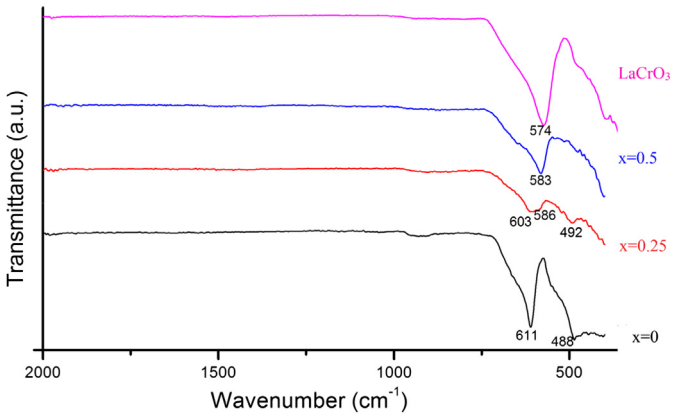

Fig. 1. IR spectra of $ZnCr_{2-x}La_xO_4$ system (x = 0, 0.25, 0.50) and $LaCrO_3$ powders.

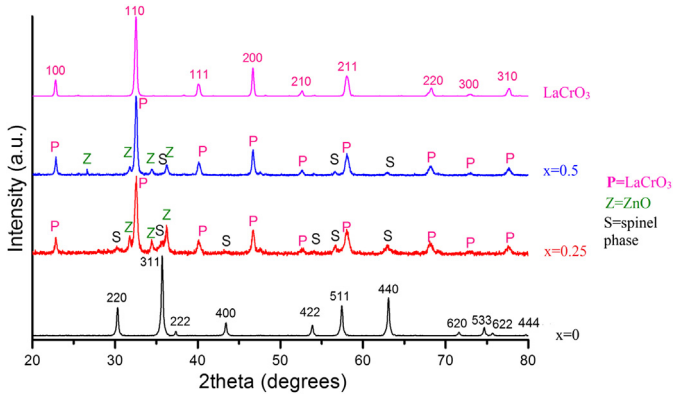

Fig. 2. X-ray diffraction patterns of $ZnCr_{2-x}La_xO_4$ (x = 0, 0.25, 0.50) and $LaCrO_3$ powders.

presence of two main absorption peaks at $\bar{\upsilon}_1$ and $\bar{\upsilon}_2$ wavenumbers, characteristic of spinel structure, for samples with La content x = 0 and x = 0.25. According to Waldron [34], the strongest absorption peak $\bar{\upsilon}_1$, observed in the range 611–603 cm^{-1}, is caused by intrinsic vibration of bonds between metal ions and oxygen ions in tetrahedral sites, whereas the weakest absorption peak $\bar{\upsilon}_2$, observed in the range 488–492 cm^{-1}, is assigned to the stretching vibrations of bonds between metal ions in octahedral sites and oxygen ions [35]. A comparison of the observed vibrational frequencies of the first two samples, indicate a decrease of the wavenumber values for tetrahedral vibrations and an increase for octahedral vibrations. The shift of $\bar{\upsilon}_2$ band to higher wavenumbers with La^{3+} content, can be attributed to the substitution of Cr^{3+} (radius: 0.615 Å) ions by La^{3+} ions (radius: 1.032 Å) in octahedral sites, which causes a decrease in the metal–oxygen bond length and an increase wavelength of absorption peaks. However, starting with the sample with La^{3+}content x = 0.25, it can be observed the appearance of the $LaCrO_3$ perovskite structure proved by the presence, at 586 cm^{-1}, of a band typical for anti-symmetric ($\bar{\upsilon}_{as}$) octahedral CrO_6 stretching vibrations [36]. Moreover, deeper substitution with higher ionic radius La cations causes the quasicomplete disparition of $\bar{\upsilon}_1$ band and a shift towards smaller wavenumber for $\bar{\upsilon}_{as}$ band (from 586 cm^{-1} and 583 cm^{-1}) probably due to the formation of perovskite-type phase in higher amounts [37,38]. Therefore, it could be noticed that the IR spectra of sample with x = 0.5 is very similar with the $LaCrO_3$ spectra, indicating that the perovskite phase became majoritary. Nevertheless, these observations must be confirmed by other analyses like X-ray diffraction.

3.2. X-ray diffraction study

The XRD patterns of as-obtained powders are shown in Fig. 2. The diffraction peaks from (220), (311), (222), (400), (422), (511) (440), (620), (533), (622) and (444) planes correspond to the spinel structure of $ZnCr_2O_4$ (JCPDS card No. 22-1107) which belonging to the Fd3m space group with cubic symmetry. It can be observed that insertion of La^{3+} in spinel lattice produces a shift of the (3 1 1) diffraction peak, and from the sample with x = 0.25, a perovskite structure [diffraction peak (1 1 0)] with cubic unit cell belonging to the Pm-3m space group [37,39] may be formed. This is confirmed by the diffraction pattern of $LaCrO_3$ (JCPDS card No. 75–0441) offered for comparison. As La^{3+} substitution increases, the deviation from spinel phase becomes more prominent with the appearance of secondary phases with significant amount of zinc oxide (ZnO: JCPDS card No. 36-1451) phase and spinel $ZnCr_2O_4$ phase (JCPDS card No. 22-1107). The formation of secondary phases in the spinel oxides during sintering process is governed by amount of La^{3+} used. Higher rare-earth content leads to a higher potential barrier for La^{3+} ion to overcome for entering into the B-site of spinel crystal lattice. It can be observed that diffraction peaks corresponding to secondary phases decrease with content of La^{3+} increases. Phases quantification (Fig. 3a–c)was estimated using FullProf 2000 program [40], by profile fitting, with a peak shape modeled by a Pseudo-Voigt function using the Thomson Cox Hastings model [41] and for instrumental profile corrections was used LaB6 as a standard for instrumental profile corrections. For $ZnCr_2O_4$ was determined a high percentage of secondary phase of ZnO, which in pattern from Fig. 2 could not be seen because probably overlaps the diffraction peak corresponding to spinel phase. For the substituted samples, the results indicate the presence of $LaCrO_3$ (antiferromagnetic) as majority phase and $ZnCr_2O_4$ and ZnO (antiferromagnetic and diamagnetic, respectively) phases in ratios reported in Table 1. One can observe that the amount of La has a significant influence on phase content which varies for $ZnCr_2O_4$ from 78% (for La x = 0) to 5% (for La x = 0.5). Therefore, the relatively large amount of La^{3+} ions in $ZnCr_2O_4$ can affect not only the phase composition but also the size of the spinel matrix. The secondary phases are probably due to the limited solubility of La in the $ZnCrO_4$ spinel lattice, which is below x = 0.25, according to our results and to literature data [30]. In our opinion, the La ions occupy either the Zn positions or go to the grain boundaries. However we have to exclude the probability that the bulky rare-earth ions occupy the B-sites of Cr^{3+} ions. This is because of the fact that the octahedral sites are too small to be occupied by the large rare-earth ions with large ionic radius. Of course the occupancy of the tetrahedral sites by the rare-earth ions is possible, leading to the formation of a new main structure, in this case, the perovskite one.

It has been reported [41] that phases formation is affected by the concentration of rare-earth element in substituted spinel oxides. This can be attributed to dimension of RE^{3+} ionic radii and electronic configuration [42]. For example, if the amount of La^{3+} is large enough, then it will form secondary phases on the grain boundaries or transitions to other types of structures will occur due to significantly larger ionic radius and diffusion of La^{3+} ions. Therefore, an explanation for the transition of spinel structure to perovskite structure is the exchange of Zn^{2+} and La^{3+} cations among A-sites, a position occupied by lanthanum ions due to very large ionic radius. Based on the above discussion, doping with small amounts of lanthanum can be achieved on octahedral B-position, but bringing a deficiency of A-site cations. When it reaches the degree of solubility, lanthanum ions will occupy only constituent A-sites through complete substitution of Zn ions, leading to the formation of a new

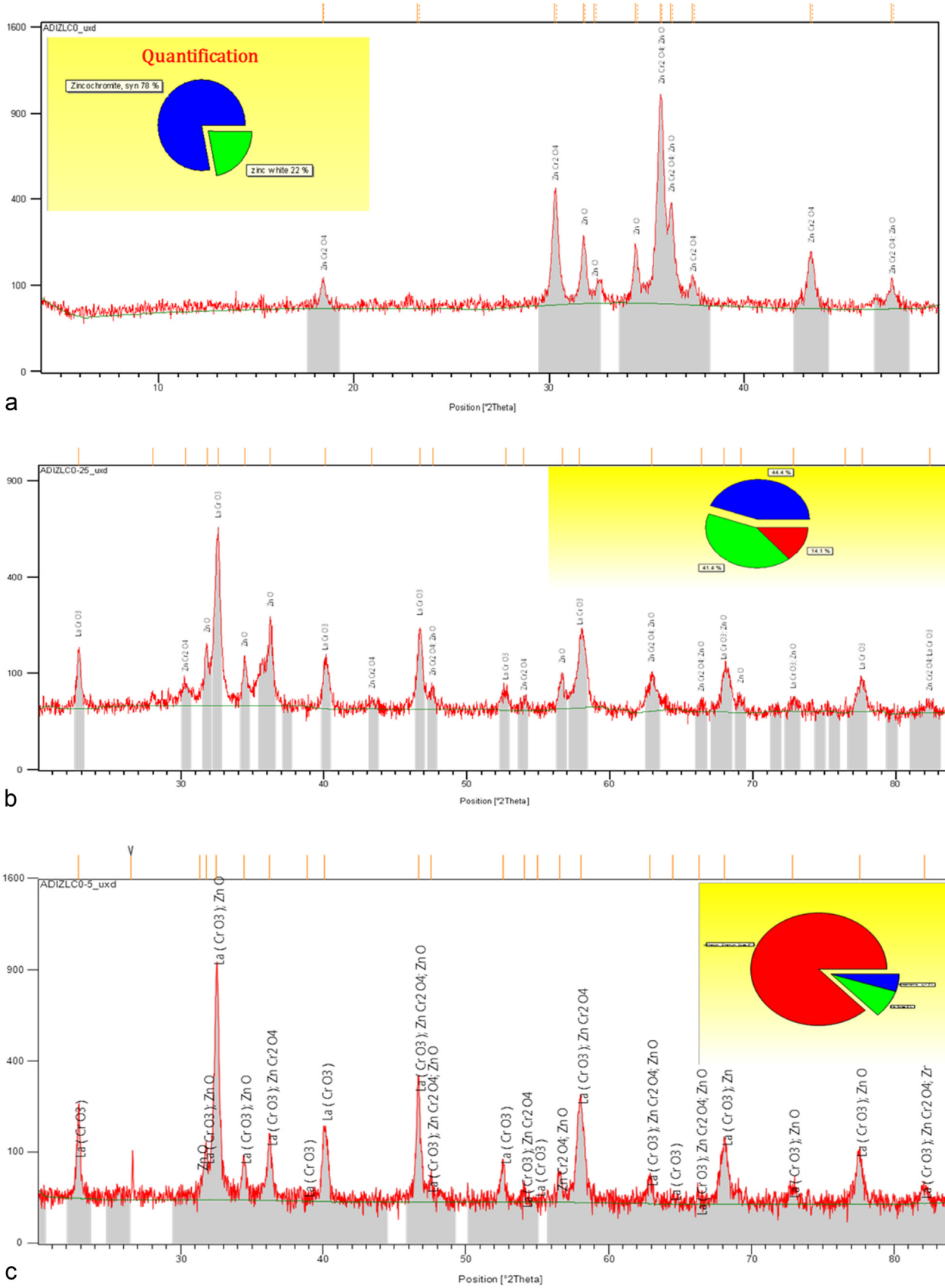

Fig. 3. (a–c). Phases quantification for samples with x = 0; 0.25 and 0.50, by profile fitting.

Table 1
Phases quantification and the profile parameters estimated using FullProf 2000 program.

Sample	Phase identification and quantification			Profile parameters		Reliability factor (χ^2)
	Chemical formula	Space group	Composition (%)	Lattice parameter (Å)	Crystallite size (nm)	
ZCL0	$ZnCr_2O_4$	*Fd-3m*	78	8.334(1)	29.4(1)	1.49
	ZnO	*P63mc*	22	*a* = 3.250(5) *c* = *5.205(9)*		
ZCL0.25	$ZnCr_2O_4$	*Fd-3m*	14	8.250(6)	28.1(3)	1.98
	$LaCrO_3$	*Pm-3m*	44	8.690(9)		
	ZnO	*P63mc*	41	*a* = 3.248 (8) *c* = *5.197(6)*		
ZCL0.5	$ZnCr_2O_4$	*Fd-3m*	5	8.248(6)	25.2(1)	3.88
	$LaCrO_3$	*Pm-3m*	87	8.698(2)		
	ZnO	*P63mc*	8	*a* = 3.248(9) *c* = *5.195(4)*		

structure, in this case, the perovskite. This transition is confirmed by crystallite size variation, estimated from Rietveld refinement. The average crystallite size decreases with phase transition, from 29.4 nm for the $ZnCr_2O_4$ to 25.2 nm for the material with La x = 0.5. XRD results mentioned in Fig. 1 confirmed that, after the addition of La ions, the main phase of the samples is $LaCrO_3$ and the grain boundary phases are $ZnCr_2O_4$ and ZnO. The decrease in crystallite size of the samples with increasing amount of La^{3+} ions can be explained on the basis of energy needed for the substituted samples to complete crystallization and growth [43]. The lattice constants of the as-prepared samples calculated from the XRD data refinement are listed in Table 1. The lattice constant dropped down when the substitution amount of La^{3+} ions increased to x = 0.5. The larger amount of $LaCrO_3$ in case of composition with x = 0.5 would cause the expansion of unit cell, resulting in larger lattice constants. However, with additional La^{3+} introduction in matrix, the lattice constants decreased. This can be attributed to that part of La^{3+} ions could not enter the octahedral site but form a phase of $LaCrO_3$, thereby causing the lattice contraction and thus the decrease in lattice constant. Similar phenomenon was also observed for La^{3+}-doped Ni–Zn ferrites obtained by a sol–gel auto-combustion method [44].

3.3. SEM analysis

SEM micrographs used to obtain further structural informations of selected samples are shown in Fig. 4 (a–d). The SEM pictures showed spherical shaped particles, and also indicated nearly uniform distribution of particles. Better grain boundaries were observed at smaller substitution of La^{3+} ions. Compared with the XRD results mentioned above, it can be confirmed that after the addition of La^{3+} ions, the main phase of the samples is $LaCrO_3$ and grain boundary phase could be spinel phase and zinc oxide. Further, it is observed that the particle size decrease with La^{3+} substitution because of the appearance of $LaCrO_3$ phase in addition to cubic phase. This $LaCrO_3$ phase indicates that the Cr^{3+} ions are not replaced by La^{3+} ions at the octahedral sites which inhibit the grain growth. The particles size, as-obtained in ImageJ program, decreases with La substitution ranging between 80 nm for $ZnCr_2O_4$ and 48 nm for x = 0.50 La content. SEM image for $LaCrO_3$ sample shows agglomerated particles with spherical shapes and average size of 80 nm. The decrease in particle size of the samples with increasing La^{3+} substitution ions can be explained as follows. The materials with rare earth ions has high thermal stability, and hence more energy is needed for the La^{3+} ions incorporation into spinel lattice, forming La^{3+}-O bond, and growth of particles, respectively [16]. In addition, the formed secondary spinel phase for samples with x = 0.25 and 0.50, pinning at the grain boundary, will hinder the growth of perovskite grains, resulting in smaller perovskite particles and thus denser materials.

3.4. Magnetic properties

Fig. 5 (a–b) shows the field dependent magnetization (M vs H) of $ZnCr_{2-x}La_xO_4$ (x = 0, 0.25, 0.50) system obtained at 2 K and 300 K. The M vs H curves for all samples measured at 300 K reveal a linear behavior to the high field region. For all the samples, the loops do not reach saturation at 6 T due to the slight non-compensated paramagnetic contribution. Note that all the materials show a similar paramagnetic behavior and the magnetization decreases with the paramagnetic La^{3+} content. The observed behavior could be attributed to crystallite size decrease with the rare-earth cations amount. As the crystallite size decreases, the surface effect becomes prominent, leading to distortions on the structure. Hence, surface atoms are under the effect of strain which leads to vacancies and a variety of interatomic spacing. All of these factors leads to spin disorder at the surface, which causes low magnetization [22]. On the other hand, the magnetization recorded at 2 K (Fig. 5b) showed small hysteresis loops to all the studied materials indicating the existence of possible superparamagnetic behaviors and surface effects which are likely due to the uncompensated spins on the sample surface. The value of magnetization at 2 K shows an anomalous behavior with La^{3+} ions substitution. One can notice that the sample with x = 0.25 shows a magnetization higher than observed for $ZnCr_2O_4$, which may be due to co-existence of several phases in the structure. So, this anomalous behavior of magnetization may be due to the formation of secondary phases i.e., $ZnCr_2O_4$ and ZnO (non-magnetic) phases as explained in X-ray diffraction analysis. The sample containing the higher La ions concentration (x = 0.5) shows an extremely small magnetization, i.e. 10 emu/g, which means that perovskite phase was stabilized and it became predominant in the network. In addition, a decreasing in the magnetic properties can be attributed to the decrease in crystallite, which indicates a direct relationship between magnetic properties and crystal growth, meaning that the decrease in magnetic parameters values may be associated with decreased crystallite size depending on the La content. A very interesting observation is that the magnetization increases at 2 K towards 300 K. For example, in the case of the sample with the content of lanthanum, x = 0.25, magnetization measured at 300 K is 28 emu/g while at 2 K is 75 emu/g. According to the literature, this variation can be described by the theory of spin waves at low temperature [45]. Therefore, the spins of the atoms are completely parallel at 2 K, but by raising the temperature, chaotic spin arrangement will increase. Hence, the value of M increases with the decrease of temperature. The zero field-cooled (ZFC) and the field-cooled (FC) magnetization curve for the unsubstituted and substituted samples at an applied field of 1 T in the temperature range of 2–300 K are given in Fig. 6. Below room temperature, all curves show almost identic reversibility. Moreover, no magnetic transitions were observed for the investigated samples in the temperature range used in measurements of this work. But *M*

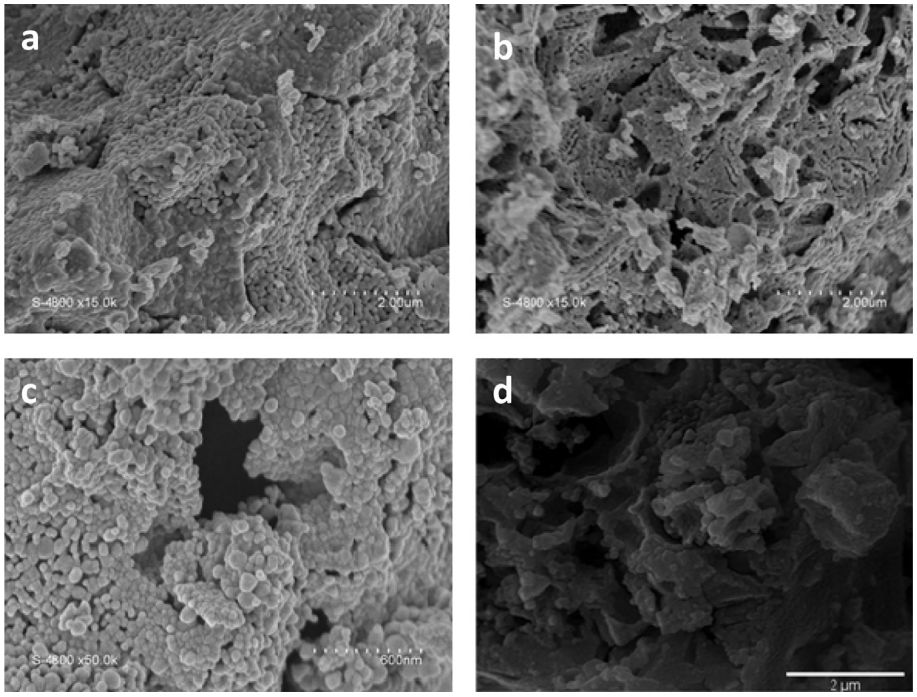

Fig. 4. SEM images of (a) x = 0, (b) x = 0.25, (c) x = 0.50 of $ZnCr_{2-x}La_xO_4$ system and (d) $LaCrO_3$.

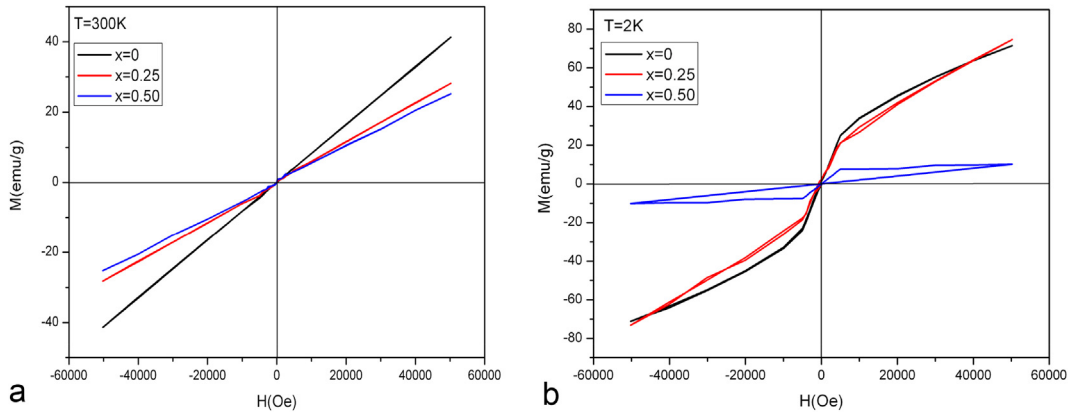

Fig. 5. Variation of magnetization (M) with applied field (H) at (a) 300 K and (b) 2 K of $ZnCr_{2-x}La_xO_4$ system (x = 0, 0.25, 0.50).

increased with decrease of temperature, suggesting that entropy of electronic spin configuration prevailed at low temperature [46]. The drastic magnetization decrease with temperature is due to the grain size decrease. This is because of the domain walls partly coincide with the grain boundaries. Therefore, the increase in grain boundaries with grain size decrease leads to the pinning of domain walls motion. As such it is assumed that magnetic ordering can be broken up easily at nonmagnetic grain boundaries and then there is only a short range magnetic exchange interaction [47]. With increase of La content, vacancy increases, resulting enhanced domain pinning effect which decrease the magnetization [48]. In this context, it seems that the drastic decrease of magnetization with temperature increase comes from structural phase transition, from $ZnCr_2O_4$ spinel in $LaCrO_3$ perovskite.

4. Conclusions

The synthesis of $ZnCr_{2-x}La_xO_4$ nano-sized spinel oxides show the formation of spinel cubic crystal structure for $ZnCr_2O_4$ with transition to perovskite structure as main phase in presence of bulky rare-earth La^{3+} ions, which cannot enter in spinel lattice.

X-ray diffraction confirmed the formation of nanosized crystallites and transition of spinel structure to perovskite structure because of the exchange of Zn^{2+} and La^{3+} cations among A-sites, a position occupied by lanthanum ions due to very large ionic radius. The occupation number of individual atoms over the A and B-sites are affected by the variation of the La^{3+} substitution. The replacement of Cr cations with bulky La cations in spinel-type materials is limited to the doping level; the substitution is practically impossible. At higher concentrations the rare-earth cations tend to form perovskite-type materials with the B-site cations. When it reaches the degree of solubility, lanthanum ions will occupy only constituent A-sites through complete substitution of Zn ions, leading to the formation of a new perovskite structure.

With increase of La content, vacancy increases, resulting enhanced domain pinning effect with decrease in magnetization,

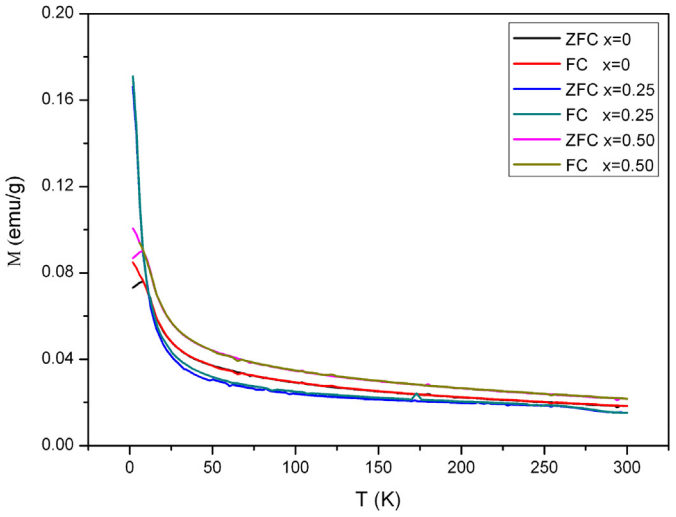

Fig. 6. Variation of magnetization (M) with temperature (T/K) under ZFC, FC at 1 T.

which seems that drastic decrease of magnetization with temperature comes from structural phase transition.

Acknowledgments

The author A.I. Borhan is grateful for the financial support of the European Social Fund in Romania, under the responsibility of the Managing Authority for the Sectoral Operational Programme Human Resources Development 2007–2013 [grant POSDRU/107/1.5/S/78342].

References

[1] A.N. Naveen, S. Selladurai, Tailoring structural, optical and magnetic properties of spinel type cobalt oxide (Co_3O_4) by manganese doping, Phys. B 457 (2015) 251–262.
[2] T. Brylewski, W. Kucza, A. Adamczyk, A. Kruk, M. Stygar, M. Bobruk, J. Dąbrowa, Microstructure and electrical properties of $Mn_{1+x}Co_{2-x}O_4 (0 \le x \le 1.5)$ spinels synthesized using EDTA-gel processes, Ceram. Int. 40 (9) (2014) 13873–13882. A.
[3] S. Dwivedi, R. Sharma, Y. Sharma, Electroconductive properties in doped spinel oxides, Opt. Mater 37 (2014) 656–665.
[4] H.-jie Zhang, J. Wang, X.-F. Xu, Catalytic decomposition of N_2O over $Ni_xCo_{1-x}CoAlO_4$ spinel oxides prepared by sol-gel method, J. Fuel Chem. Techn 43 (1) (2015) 81–87.
[5] Y. Zhang, J. Rosen, G.S. Hutchings, F. Jiao, Enhancing photocatalytic oxygen evolution activity of cobalt-based spinel nanoparticles, Catal. Today 225 (2014) 171–176.
[6] X. Niu, W. Du, W. Du, Preparation and gas sensing properties of ZnM_2O_4 (M = Fe, Co, Cr), Sens. Actuators B Chem. 99 (2004) 405–409.
[7] L. Mancic, Z. Marinkovic, P. Vulic, C. Moral, O. Milosevic, Morphology, structure and nonstoichiometry of $ZnCr_2O_4$ nanophased powder, Sensors 3 (2003) 415–423.
[8] S. Pokhrel, B. Jeyaraj, K.S. Nagaraja, Humidity-sensing properties of $ZnCr_2O_4$–ZnO composites, Mater. Lett. 57 (22–23) (2003) 3543–3548.
[9] S. Boumaza, A. Bouguelia, R. Bouarab, M. Trari, physical and photoelectrochemical studies for hydrogen photo-evolution over the spinel $ZnCr_2O_4$, J. Int. Hydrogen Energy 34 (2009) 4963–4967.
[10] C. Peng, L. Gao, Optical and photocatalytic properties of spinel $ZnCr_2O_4$ nanoparticles synthesized by a hydrothermal route, J. Am. Ceram. Soc. 91 (2008) 2388–2390.
[11] E. Kojima, A. Miyata, Y. Motome, H. Ueda, Y. Ueda, S. Takeyama, Magnetic orders of highly frustrated spinel, $ZnCr_2O_4$ in magnetic fields up to 400 T, J. Low. Temp. Phys. 159 (2010) 3–6.
[12] A.I. Borhan, T. Slatineanu, A.R. Iordan, M.N. Palamaru, Influence of chromium ion substitution on the structure and properties of zinc ferrite synthesized by the sol–gel auto-combustion method, Polyhedron 56 (2013) 82–89.
[13] S.E. Dutton, Q. Huang, O. Tchernyshyov, C.L. Broholm, R.J. Cava, Sensitivity of the magnetic properties of the $ZnCr_2O_4$ and $MgCr_2O_4$ spinels to non-stoichiometry, Phys. Rev. B 83 (064407) (2011) 16.
[14] Y. Xue, S. Naher, F. Hata, H. Kaneko, H. Suzuki, Y. Kino, Low temperature X-ray diffraction study of $ZnCr_2O_4$ and $Ni_{0.5}Zn_{0.5}Cr_2O_4$, J. Low. Temp. Phys. 151 (2008) 1193–1204.
[15] O.M. Hemeda, M.Z. Said, M.M. Barakat, Spectral and transport phenomena in Ni ferrite-substituted Gd_2O_3, J. Magn. Magn. Mater 224 (2) (2001) 132–142.
[16] K.S. Lohar, A.M. Pachpinde, M.M. Langade, R.H. Kadam, Sagar E. Shirsath, Self-propagating high temperature synthesis, structural morphology and magnetic interactions in rare earth Ho^{3+} doped $CoFe_2O_4$ nanoparticles, J. Alloys Compd. 604 (2014) 204–210.
[17] K.K. Bamzai, G. Kour, B. Kaur, S.D. Kulkarni, Effect of cation distribution on structural and magnetic properties of Dy substituted magnesium ferrite, J. Magn. Magn. Mater 327 (2013) 159–166.
[18] P. Samoila, L. Sacarescu, A.I. Borhan, D. Timpu, M. Grigoras, N. Lupu, M. Zaltariov, V. Harabagiu, Magnetic properties of nanosized Gd doped Ni–Mn–Cr ferrites prepared using the sol–gel autocombustion technique, J. Magn. Magn. Mater 378 (2015) 92–97.
[19] A.A. Kadam, S.S. Shinde, S.P. Yadav, P.S. Patil, K.Y. Rajpure, Structural, morphological, electrical and magnetic properties of Dy doped Ni–Co substitutional spinel ferrite, J. Magn. Magn. Mater 329 (2013) 59–64.
[20] P. Samoila, T. Slatineanu, P. Postolache, A.R. Iordan, M.N. Palamaru, The effect of chelating/combustion agent on catalytic activity and magnetic properties of Dy doped Ni-Zn ferrite, Mater. Chem. Phys. 136 (1) (2012) 241–246.
[21] R.D. Shannon, Revised effective ionic radii and systematic studies of interatomic distances in halides and chalcogenides, Acta Crystallogr. A32 (1976) 751–767.
[22] L. Kumar, M. Kar, Effect of La^{3+} substitution on the structural and magneto-crystalline anisotropy of nanocrystalline cobalt ferrite ($CoFe_2-xLaxO_4$), Ceram. Int. 38 (6) (2012) 4771–4778.
[23] P. Kumar, S.K. Sharma, M. Knobel, M. Singh, Effect of La^{3+} doping on the electric, dielectric and magnetic properties of cobalt ferrite processed by co-precipitation technique, J. Alloys Compd. 508 (1) (2010) 115–118.
[24] M.T. Rahman, M. Vargas, C.V. Ramana, Structural characteristics, electrical conduction and dielectric properties of gadolinium substituted cobalt ferrite, J. Alloys Compd. 617 (2014) 547–562.
[25] Z. Peng, X. Fu, H. Ge, Z. Fu, C. Wang, L. Qi, H. Miao, Effect of Pr^{3+} doping on magnetic and dielectric properties of Ni–Zn ferrites by "one-step synthesis", J. Magn. Magn. Mater 323 (20) (2011) 2513–2518.
[26] X. Wu, W. Wu, L. Qin, K. Wang, S. Ou, K. Zhou, Y. Fan, Structure and magnetic properties evolution of nickel–zinc ferrite with lanthanum substitution, J. Magn. Magn. Mater 379 (2015) 232–238.
[27] M. Yehia, S.M. Ismail, A. Hashhash, Structural and magnetic studies of rare-earth substituted nickel ferrites, J. Supercond. Nov. Magn. 27 (2014) 771–774.
[28] E. Rezlescu, N. Rezlescu, P.D. Popa, Fine-grained MgCu ferrite with ionic substitutions used as humidity sensor, J. Magn. Magn. Mater. 290–291 (2005) 1001–1004.
[29] M.A. Ahmed, N. Okasha, M.M. El-Sayed, Enhancement of the physical properties of rare-earth-substituted Mn–Zn ferrites prepared by flash method, Ceram. Int. 33 (1) (2007) 49–58.
[30] P.K. Roy, J. Bera, Enhancement of the magnetic properties of Ni–Cu–Zn ferrites with the substitution of a small fraction of lanthanum for iron, Mater. Res. Bull. 42 (2007) 77–83.
[31] J. Sun, J. Li, G. Sun, Effects of La_2O_3 and Gd_2O_3 on some properties of Ni–Zn ferrite, J. Magn. Magn. Mater 250 (2002) 20–24.
[32] A. Gadkari, T. Shinde, P. Vasambekar, Influence of rare-earth ions on structural and magnetic properties of $CdFe_2O_4$ ferrites, Rare Met. 29 (2) (2010) 168–173.
[33] E. Melagiriyappa, M. Veena, A. Somashekarappa, G.J. Shankaramurthy, H.S. Jayanna, Dielectric behavior and ac electrical conductivity in samarium substituted Mg–Ni ferrites, Indian J. Phys. 88 (8) (2014) 795–801.
[34] R.D. Waldron, Infrared Spectra of Ferrites, Phys. Rev. 99 (1955) 1727–1735.
[35] H. Cui, M. Zayat, D. Levy, Sol–gel synthesis of nano- scaled spinels using propylene oxide as a gelation agent, J. Sol Gel Sci. Technol. 35 (2005b) 175–181.
[36] N. Soltani, S.M. Hosseini, A. Kompany, Nanoscale ab-initio calculations of optical and electronic properties of $LaCrO_3$ in cubic and rhombohedral phases, Phys. B 404 (2009) 4007–4014.
[37] K. Rida, A. Benabbas, F. Bouremmad, M.A. Peña, E. Sastre, A. Martinez-Arias, Effect of calcination temperature on the structural characteristics and catalytic activity for propene combustion of sol–gel derived lanthanum chromite perovskite, Appl. Catal. A 327 (2007) 173–179.
[38] G.A. Tompsett, N.M. Sammes, Characterisation of the SOFC material, $LaCrO_3$, using vibrational spectroscopy, J. Power Sources 130 (2004) 1–7.
[39] K. Tezuka, Y. Hinatsu, A. Nakamura, T. Inami, Y. Shimojo, Y. Morii, Magnetic and neutron diffraction study on perovskites $La_{1-x}Sr_xCrO_3$, J. Solid State Chem. 141 (1998) 404.
[40] Rodriguez Carvajal, Recent advances in magnetic structure determination by neutron powder diffraction, Phys. B Cond. Matter 192 (1993) 55–69.
[41] P. Thompson, D.E. Cox, J.B. Hastings, Rietveld refinement of Debye-Scherrer synchrotron X-ray data from Al_2O_3, J. Appl. Crystallogr. 20 (1987) 79–83.
[42] E. Ateia, M.A. Ahmed, A.K. El-Aziz, Effect of rare earth radius and concentration on the structural and transport properties of doped Mn–Zn ferrite, J. Magn. Magn. Mater 311 (2007) 545–554.
[43] N. Rezlescu, E. Rezlescu, C. Pasnicu, M.L. Craus, Effects of the rare-earth ions on some properties of a nickel–zinc ferrite, J. Phys. Condens. Matter 6 (1994) 5707–5716.
[44] X.H. Ren, G.L. Xu, Electromagnetic and microwave absorbing properties of NiCoZn-ferrites doped with La^{3+}, J. Magn. Magn. Mater 354 (2014) 44–48.
[45] L. Zhao, H. Yang, L. Yu, Y. Cui, X. Zhao, S. Feng, Study on magnetic properties of

nanocrystalline La-, Nd-, or Gd-substituted Ni–Mn ferrite at low temperatures, J. Magn. Magn. Mater 305 (2006) 91–94.
[46] Y. Matsunaga, F. Nakamura, H. Takahashi, T. Hashimoto, Analysis of relationship between magnetic property and crystal structure of $La_{1-x}Sr_xCrO_3$ ($x = 0.13, 0.15$), Solid State Commun. 145 (2008) 502–506.
[47] Kashif Ali, A.K. Sarfraz, Atif Ali, A. Mumtaz, S.K. Hasanain, Temperature dependence magnetic properties and exchange bias effect in $CuFe_2O_4$ nanoparticles embedded in NiO matrix, J. Magn. Magn. Mater 369 (2014) 81–85.
[48] K. Kamala Bharathi, G. Markandeyulu, C.V. Ramana, Structural, magnetic, electrical, and magnetoelectric properties of Sm- and Ho-substituted nickel ferrites, J. Phys. Chem. C 115 (2) (2011) 554–560.